Vol 17 No 12, December 2008
1674-1056/2008/17(12)/4656-09

Chinese Physics B

© 2008 Chin. Phys. Soc.
and IOP Publishing Ltd

Optical parameters and energy levels splitting of Ho^{3+} in Ho^{3+}: $GdVO_4$*

Wang Ce(王　策)[a], Chen Xiao-Bo(陈晓波)[a]†, Zhang Chun-Lin (张春林)[b], Zhang Yun-Zhi(张蕴芝)[b], Liu Jin-Ying(刘金英)[a], Wang Ya-Fei (王亚非)[a], Liu Da-He(刘大禾)[a], Du Shuai(杜　帅)[b], Xu Xiao-Ling(徐小灵)[a], Wang Lei(王　磊)[a], and Li Song(李　崧)[a]

[a] *Applied Optics Beijing Area Major Laboratory, Department of Physics, Analysis and Testing Center, Beijing Normal University, Beijing* 100875, *China*
[b] *Institute of Physics Chinese Academy of Sciences, Beijing* 100190, *China*

(Received 21 May 2008; revised manuscript received 19 July 2008)

$Ho^{3+}:GdVO_4$ is a new laser material suitable for high-power laser systems. In this paper we measure the absorption spectra of Ho^{3+} in the sample Ho^{3+}: $GdVO_4$. The intensity parameters are calculated by using the Judd–Ofelt theory. Some predicted spectroscopic parameters, such as the spontaneous radiative transition rate, branching ratio and integrated emission cross section are dealt with. And we also compare the optical parameters with those of other materials. From these results, it is found that there are many transitions which have large oscillator strengths and large integrated emission cross sections. Especially the transitions such as $^5F_4 \rightarrow {}^5I_8$, $^5S_2 \rightarrow {}^5I_8$, $^5F_5 \rightarrow {}^5I_8$ and $^5I_7 \rightarrow {}^5I_8$ are useful in solid-state lasers and other fields. Finally, we discuss the splitting of the energy levels of Ho^{3+} in the crystal $GdVO_4$ based on the group theory.

Keywords: Ho^{3+}: $GdVO_4$, absorption spectrum, intensity parameters, laser material
PACC: 7840, 3270

1. Introduction

Holmium ion has abundant luminescence phenomena due to its special energy level distribution, especially sensitized by Yb^{3+} and Tm^{3+} ions in up-conversion luminescence.[1−8] And its high efficiency has attracted many researchers' attention. Ho^{3+}, as an activator, not only can emit green and red light but also can lase in an eye safe range at $2\,\mu$m corresponding to $^5I_7 \rightarrow {}^5I_8$ transition.[9,10,11] which can be applied in the field of medicine, laser radar, underwater exploration etc. In addition, the development of near infrared laser in chemistry, laser measurement, non-linear laser spectroscopy, etc makes the materials doped with Ho^{3+} investigated more widely.[12−17]

$GdVO_4$ crystal as the host of RE^{3+} was first introduced by Zaguniennyi *et al* in 1992.[18] They found that $GdVO_4$ crystal had a higher thermal conductivity, a larger absorption cross section and a larger emission cross-section than YVO_4 crystal which was considered to be suitable for a laser material. Besides these advantages, many other features such as a high chemical stability, etc also have attracted a great many of researchers.[19] $GdVO_4$ crystal is a tetragonal system similar to YVO_4, and belongs to the space group I41/amd. Some of Gd^{3+} ions are replaced by Ho^{3+} ions in a Ho^{3+}:$GdVO_4$laser crystal and the symmetry of Ho^{3+} belongs to the group D_{2d}. Lattice parameters are $a = b = 0.7212\,$nm, and $c = 0.63483\,$nm.

In this paper, we firstly measure the absorption spectra of Ho^{3+} in the sample $Ho^{3+}:GdVO_4$, then calculate the intensity parameters using Judd–Ofelt (J-O) theory.[20,21] After that we deal with some predicted spectroscopic parameters, such as the spontaneous radiative transition rate, branching ratio and integrated emission cross section. Finally, we discuss the splitting of the energy levels of Ho^{3+} in the crystal $GdVO_4$ by using the group theory.

2. Experiments

The $Ho^{3+}:GdVO_4$ crystal with good optical quality is grown by using the Czochralski method. The concentration of Ho^{3+} in the $GdVO_4$ crystal discussed

*Project supported by the National Natural Science Foundation of China (Grant No 10174008).
†Corresponding author. E-mail: xbchen@bnu.edu.cn

in this paper is 1 mol%, which is analysed by using the inductively coupled plasma (ICP) analytical method. The size of the crystal is 5 mm×7 mm×10 mm. The c-axis is in the direction of the 5 mm side, and a-axis is in the direction of the 7 mm side. The density of the sample is 5.37 g/cm^3, and its refractive index is 1.972. We measure the absorption spectra in the c-axis and the a-axis directions separately by using the UV-365 spectrophotometer at room temperature, which are shown in Figs.1 and 2. The solid line represents the absorption spectrum in the c-axis direction, and the dotted line refers to the absorption spectrum in the a-axis direction. In Figs.1 and 2, the absorption peaks from right to left correspond to the transitions from the ground state $^5I_8$ of Ho^{3+} to the excited states $^5I_7$, $^5I_6$, $^5I_5$, $^5I_4$, $^5F_5$, $^5S_2$, $^5F_4$, $^5F_3$, $^5F_2$, $^3K_8$, $^5G_6$, $^5F_1$, $^5G_5$, $^5G_4$, $^3K_7$, $^3G_5$, and $^3H_6$ respectively. Because the experiments are performed at room temperature, some absorption peaks are hardly distinguishable from each other, such as $^5S_2$ and $^5F_4$, $^5F_2$ and $^3K_8$. So we

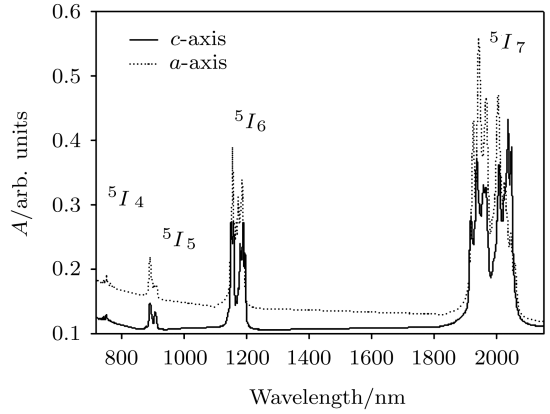


Fig.1. Absorption spectra of $Ho^{3+}:GdVO_4$ in the c-axis and the a-axis directions (720–2150 nm).

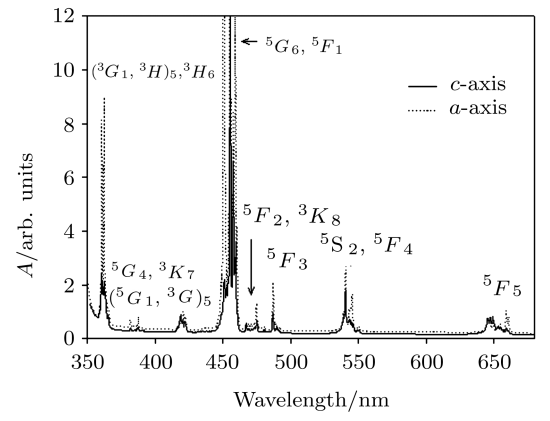


Fig.2. Absorption spectra of $Ho^{3+}:GdVO_4$ in the c-axis and the a-axis directions (350–680 nm).

will treat them as one peak separately later. In addition, the absorption of the $GdVO_4$ host submerges the absorption of the excited states of Ho^{3+} ion which are higher than $^3H_6$, but the host absorption is small from 400 nm to infrared and does not vary acutely.

3. Calculation of optical parameters

Because the parities of the $4f^n$ configuration in free RE^{3+} ions are the same, the electric-dipole transitions between energy states are forbidden. But the odd terms of the Hamiltonian of the weak crystal field make the excited configuration $4f^{n-1}n'l'$ mix into the $4f^n$ to form the mixture of two configurations, which makes the electric-dipole transitions possible. So the transitions between energy states in the $4f^n$ configuration of the Ho^{3+} are mostly composed of the electric-dipole transition, the magnetic-dipole transition and the electric-quadruple transition. The electric-quadruple oscillator strength is much smaller than the total oscillator strength, so we neglect its contribution. Then the total oscillator strength equals the sum of the electric-dipole and the magnetic-dipole oscillator strength, which can be written as

$$f = f_{\mathrm{ed}} + f_{\mathrm{md}}. \tag{1}$$

The total oscillator strength of each excited states can be calculated from the absorption spectra which are shown in Figs.1 and 2, by using the relationship between the area under the absorption line and the oscillator strength. In the J-O theory, the electric-dipole oscillator strength is expressed as a sum of the products of the optical parameters Ω_{t} and the square of the matrix elements of the unit tensor operators $U^{(\mathrm{t})}$. The values of $U^{(\mathrm{t})}$ have little change with the ion environment, so we adopt the values reported in Ref.[22]. The magnetic-dipole oscillator strength f_{md} can be computed from the magnetic dipole, by using the Winger–Eckart theory and the intermediate coupling wave functions.[23]

Because the spin-orbit coupling interaction of rare earth ions is strong, we should take it together with the coulomb interaction into account when calculating the wave function of ions. The wave function should include those states which have the same value of J, but different values of L and S, that is to say, the wave function of the Ho^{3+} ion in the crystal, which we call the intermediate coupling function, can be expressed as the linear combination of some RS states.[24] Although ions in different environments can lead to dif-

ferent intermediate coupling functions, the physical quantities are not sensitive to the wave functions.[24] So we usually use the known intermediate coupling constants to discuss some questions in different materials. The values of these constants, adopted in this paper, can be found in Ref.[25].

According to expression (1), the electric-dipole oscillator strength can be calculated by subtracting the magnetic-dipole oscillator strength from the total oscillator strength. Then from the relationship between the electric-dipole oscillator strength and the intensity parameters we can fit the intensity parameters $\Omega_{\rm t}$ by using the least square method. Further, according to the J-O theory, we can recalculate the electric-dipole oscillator strength and give the computational value of the total oscillator strength $f^{\rm cal}$, which can be compared with the experimental value $f^{\rm exp}$. And the mean square deviation $\delta_{\rm rms}$ shown in expression (2) is used to examine the deviation of the results, where P is the number of transitions.

$$\delta_{\rm rms} = \left[\frac{\sum\limits_{i}(f_i^{\rm exp} - f_i^{\rm cal})^2}{P-3}\right]^{1/2}. \tag{2}$$

Finally, by using intensity parameter $\Omega_{\rm t}$ and the matrix elements of the unit tensor operator $\left|\left\langle - \left\| U^{(\rm t)} \right\| - \right\rangle\right|^2$ reported in Ref.[22], we can calculate the oscillator strength $f_{\rm JJ'}$ between excited states, spontaneous radiative transition rate, branching ratio and integrated emission cross section which is expressed as

$$\sum_{\rm JJ'} = \frac{\lambda^2}{8\pi n^2 c} A_{\rm JJ'}. \tag{3}$$

4. Results and analyses

We first calculate the total oscillator strength according to the absorption spectrum and fit the intensity parameters of Ho^{3+} ion by using the J-O theory. Because the absorption strength of excited state $^5G_6$ is so strong that it exceeds the working range of the spectrophotometer, we do not adopt the data of $^5G_6$ during the calculation in order to obtain more accurate intensity parameters. But the calculated value $f^{\rm cal}$ of $^5G_6$ can be achieved with the intensity parameters which have been computed and listed in Table 1. In addition, some absorption peaks such as peaks of $^5S_2$ and $^5F_4$, $^5F_2$ and $^3K_8$, $^5G_4$ and $^3K_7$, $(^3G, ^3H)_5$ and $^3H_6$ are too close to be distinguishable from each other at room temperature, so we deal with them as one peak separately which are shown in first row of Table 1. The results in the *c*-axis direction are listed in Table 1 including the experimental value $f^{\rm exp}$ and the computational value $f^{\rm cal}$ of the total oscillator strength, intensity parameters $\Omega_{\rm t}$, etc.

Table 1. Intensity parameters and oscillator strengths of Ho^{3+} in $Ho^{3+}:GdVO_4$ crystal.

Energy states	Wavelength/nm	Spectral range/nm	$f^{\rm exp}/10^{-6}$	$f^{cal}/10^{-6}$	Deflection/10^{-6}
$^5I_7$	1985.9	1814.3–2147	3.101	3.424	–0.323
$^5I_6$	1171.6	1112.3–1234.3	1.814	2.005	–0.191
$^5I_5$	898.24	856.55–938.55	0.397	0.350	0.046
$^5I_4$	753.63	724.76–779.2	0.094	0.028	0.066
$^5F_5$	649.23	624.42–676.42	6.589	6.315	0.274
$^5S_2$,$^5F_4$	541.42	525–562.2	8.958	7.346	1.613
$^5F_3$	487.71	482.5–501.8	2.933	1.930	1.004
$^5F_2$,$^3K_8$	472.88	465.8–482.5	4.032	3.864	0.168
$^5G_6$,$^5F_1$	454.8	430.13–463.8		105.535	
$(^5G$,^{3}G$)_5$	419.43	408.08–427.68	6.718	7.647	–0.928
$^5G_4$,$^3K_7$	386.59	379.84–394.03	1.497	1.477	0.020
$(^3G$,^{3}H$)_5$,^{3}H$_6$	361.78	356.2–367.8	21.387	21.179	0.208
$\Omega_2/10^{-20}$ cm^2			22.458		
$\Omega_4/10^{-20}$ cm^2			4.818		
$\Omega_6/10^{-20}$ cm^2			2.182		
RMS/10^{-6}			0.772		

The results in the a-axis direction are $\Omega_2 = 36.09 \times 10^{-20}\,\mathrm{cm}^2$, $\Omega_4 = 2.930 \times 10^{-20}\,\mathrm{cm}^2$, $\Omega_6 = 1.859 \times 10^{-20}\,\mathrm{cm}^2$, and root mean square (RMS) = 1.077×10^{-6}.

According to these results which are calculated from the data of excited states except for the $^5G_6$, the most important feature is the big value of Ω_2. From these intensity parameters fitted above, we can recalculate the oscillator strengths of $^5G_6$ which are 105.535×10^{-6} in the c-axis direction, and 157.86×10^{-6} in the a-axis direction respectively. By comparing with the results of the other excited states, we can find that the oscillator strength of $^5G_6$ is very strong, which is coincident with the feature of absorption spectrum no matter in which axial direction it is. Because the absorption strength of the excited state $^5G_6$ is so strong that it exceeds the working range of the spectrophotometer: the absorption peak of $^5G_6$ in the absorption spectrum is just part of the real absorption peak. And we cannot obtain the experimental value directly. But we can conservatively estimate the range of the oscillator strength of $^5G_6$ according to the proportional relationship between the oscillator strength and the area under the absorption line, which is larger than 70×10^{-6} in the c-axis direction and larger than 117×10^{-6} in the a-axis direction. And obviously our computational values of these oscillator strengths lie in the estimated range in both directions.

In Table 1, we can note that the oscillator strength of the excited state $^3H_6$ is also very strong except for the $^5G_6$. (The contributions to the absorption of $^5F_1$ and $(^3G,^3H)_5$ are small for their small unit tensor operators.) The transitions from the ground state $^5I_8$ to the excited states $^5G_6$ and $^3H_6$ separately are hypersensitive transitions of Ho^{3+} ions. The absorption intensities of these transitions vary acutely with host species. In other words, the magnitudes of these transitions are sensitive to the environment of Ho^{3+} ions. In addition, these transitions have characteristics of the large value of unit tensor operator $U^{(2)}$ and often come with much different values of Ω_2 in different materials.

Now we can compare the results obtained from different Ho^{3+}-doped materials to further discuss the transitions. Listed in Table 2 are some J-O intensity parameters of Ho^{3+} doped materials. We can note that the value of Ω_2 varies greatly in different materials and the value of Ω_2 in this work is the largest. Take the lead-zinc-borate glass as an example, which has nearly the same concentration of Ho^{3+} ions as ours,[26] the oscillator strength of $^5G_6$ is only 22.27×10^{-6} in this material, which is very different from the magnitude listed in Table 1. And the value of Ω_2 in this glass is also much smaller than that of Ω_2 in our $GdVO_4$ crystal. From the aspect of Ω_2, the large values of Ω_2 in the results of both directions in our work are coincident with the much larger absorptions of $^5G_6$.

Moreover we can make a comparison between the results in the two directions of our sample. As shown in the absorption spectrum, in a-axis the absorption peak of $^5G_6$ is much higher than that in the c-axis direction. Correspondingly it is natural that the $\Omega_2 = 36.09\times10^{-20}\,\mathrm{cm}^2$ in the a-axis direction is much larger than the $\Omega_2 = 22.458 \times 10^{-20}\,\mathrm{cm}^2$ in the c-axis direction. In fact, not only the absorption of the $^5G_6$ but also the absorptions of the other excited states in the a-axis direction are stronger than those in the c-axis direction. Figure3 shows a comparison between the absorption peaks of the excited states $^5S_2$ and $^5F_4$ in the two directions as an example. It is found that the absorption intensities of $^5S_2$ and $^5F_4$ in the a-axis direction are stronger than those in the c-axis direction, which is just inconspicuous as the difference of $^5G_6$ in the two directions.

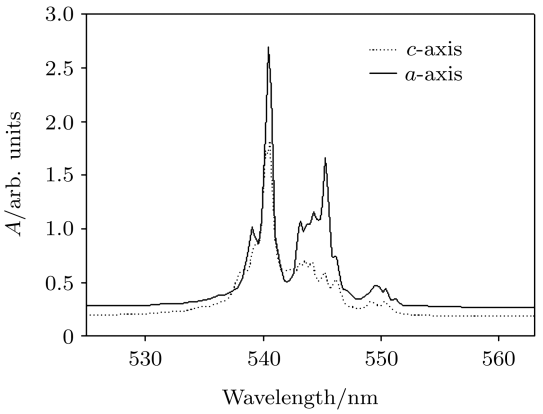


Fig.3. A comparison between the absorptions of $^5S_2$ and $^5F_4$ in the two directions.

The magnitude of Ω_6 is also noticeable. Jørgenson and Reisfeld have ever studied these three J-O intensity parameters in different rare earth ions doped materials.[27] They pointed out that the value of Ω_6 was relative to the rigidity of the host. From this point of view, the results in the c-axis and the a-axis directions in this work, i.e. $\Omega_6 = 2.182 \times 10^{-20}\,\mathrm{cm}^2$ and $1.859\times10^{-20}\,\mathrm{cm}^2$, are close to the $\Omega_6 = 1.836 \times 10^{-20}\,\mathrm{cm}^2$ in YVO_4 crystal reported in Ref.[28], which is coincident with the strong similarity between the structures of YVO_4 crystal and $GdVO_4$ crystal.

Yang *et al*[29] and Xu *et al*[30] have ever reported

the intensity parameters of Ho^{3+} in Ho^{3+}:$GdVO_4$ crystal. But their results are different from ours. And the J-O parameters in these two references are also quite different.

As analysing an anisotropy uniaxial crystal, we need to average the results in every direction in the whole space subject to using the J-O theory.[31] When the unpolarized light is incident at an arbitrary angle with respect to the optical axis, the transmitted light intensity $I_{\rm t}$ can be expressed in spherical coordinate as[31]

$$\begin{aligned} & I_{\rm t}(\lambda;\theta,\varphi) \\ = & \frac{1}{2}\sin^2\theta\cdot I_0\exp[-\alpha_\pi(\lambda)L] \\ & +\frac{1}{2}(1+\cos^2\theta)\cdot I_0\exp[-\alpha_\sigma(\lambda)L], \end{aligned} \tag{4}$$

where λ and I_0 are the wavelength and the intensity of incident light respectively; θ is the colatitude angle and φ is the azimuth angle between the light and the optical axis; L is the transit distance of light in crystal; $\alpha_\pi(\lambda)$ and $\alpha_\sigma(\lambda)$ are the rare earth ion's absorption coefficients of π transition and σ transition at the wavelength λ respectively.

When the unpolarized light propagates along the optical axis, $\theta = 0$, the transmitted light intensity is $I_0\exp[-\alpha_\sigma(\lambda)L]$. In our sample, the direction of c-axis is the direction of optical axis. Thus when the light propagates along the c-axis, there occurs only σ absorption transition. When the light propagates perpendicularly to the optical axis, $\theta = \pi/2$, which corresponds to the light transiting along a-axis in our sample, then we have $I_t(\lambda) = \frac{1}{2}I_0\{\exp[-\alpha_\pi(\lambda)L] + \exp[-\alpha_\sigma(\lambda)L]\}$. The absorption spectrum in the a-axis direction includes the compositions of σ absorption and π absorption. Because we have known the σ absorption from the results in the c-axis direction, we can calculate the π absorption further according to the above expression. The intensity parameters and the mean square deviation in π absorption of our sample are $\Omega_2 = 35.978\times10^{-20}\,{\rm cm}^2$, $\Omega_4 = 1.573\times10^{-20}\,{\rm cm}^2$, $\Omega_6 = 3.744\times10^{-20}\,{\rm cm}^2$, and RMS $= 0.541\times10^{-6}$.

According to expression (4), the average intensity of transmitted light in the whole space can be expressed as

$$\begin{aligned} & I_{\rm t}(\lambda) \\ = & \int I_{\rm t}(\lambda;\theta,\varphi){\rm d}\Omega\left(\int{\rm d}\Omega\right)^{-1} \\ = & I_0\left\{\frac{1}{3}\exp[-\alpha_\pi(\lambda)L]+\frac{2}{3}\exp[-\alpha_\sigma(\lambda)L]\right\}. \end{aligned} \tag{5}$$

For an anisotropy uniaxial crystal, a characteristic parameter can be defined as

$$\begin{aligned} \Gamma = & \lim_{L\to0}\left[-\frac{1}{L}\int\ln[\frac{I_t(\lambda)}{I_0}]{\rm d}\lambda\right] \\ = & \frac{1}{3}\int\alpha_\pi(\lambda){\rm d}\lambda+\frac{2}{3}\int\alpha_\sigma(\lambda){\rm d}\lambda \end{aligned} \tag{6}$$

to describe the absorption characteristics. It is easy to find that under this definition, the effective J-O intensity parameters of anisotropy uniaxial crystal is $\Omega_{\rm eff} = (\Omega_\pi + 2\Omega_\sigma)/3$. About our material, $\Omega_{eff2} = 26.965\times10^{-20}\,{\rm cm}^2$, $\Omega_{\rm eff4} = 3.736\times10^{-20}\,{\rm cm}^2$, and $\Omega_{\rm eff6} = 2.703\times10^{-20}\,{\rm cm}^2$ are obtained.

In Ref.[29], the author gave the effective intensity parameters as $\Omega_2 = 1.51\times10^{-20}\,{\rm cm}^2$, $\Omega_4 = 1.61\times10^{-20}\,{\rm cm}^2$, and $\Omega_6 = 1.22\times10^{-20}\,{\rm cm}^2$. We can also calculate the effective intensity parameters from the results of π absorption and σ absorption in Ref.[30], which are $\Omega_2 = 8.1701\times10^{-20}\,{\rm cm}^2$, $\Omega_4 = 10.9939\times10^{-20}\,{\rm cm}^2$, and $\Omega_6 = 2.7669\times10^{-20}\,{\rm cm}^2$. Considering the results in this paper, we find that the intensity parameters change greatly.

The intensity parameters, which are exactly computed from the absorption spectrum, are related to the properties of the sample. So the differences among intensity parameters must be reflected in absorption spectrum. From Figs.1 and 2, we can note that the absorption of our $GdVO_4$ host is small no matter in which axial direction of the crystal it is, and the fine structures of many absorption peaks can be seen, which reflect the high quality of our sample. The main difference in absorption spectrum between ours and those from other two papers is that our relative absorption intensity of the excited state $^5G_6$ is much higher than those reported in Refs.[29, 30]. And this difference in hypersensitive transition absorption is accordant with the big differences in intensity parameter especially in value of Ω_2. There are several factors that may lead to these big differences, such as the distinctions in preparing the samples, different concentrations of Ho^{3+} and so on. Especially the difference in fabrication process can affect the structural integrity of material, which may be reflected from x-ray diffraction spectrum as a little different peak position, different peak intensity and impure peaks. It means that the environment of Ho^{3+} ions is different. Moreover, these influences are related to the intensity of the covalent bonding. According to the study by Jørgenson and Reisfeld, the Ω_2 parameter is strongly affected by chemical covalent bonding. Thus through comparing, we can note that the transitions of Ho^{3+} ion in $GdVO_4$ crystals are sensitive to the environment of Ho^{3+} ions.

Table 2. A comparison among Judd-Ofelt intensity parameters for Ho^{3+} in different hosts.

	$\Omega_2/10^{-20}\mathrm{cm}^2$	$\Omega_4/10^{-20}\mathrm{cm}^2$	$\Omega_6/10^{-20}\mathrm{cm}^2$	Reference
$NaGd(WO_4)_2$	9.12	4.73	0.86	[32]
$LiNbO_3$	4.30	5.11	1.89	[33]
YAG	0.04	2.67	1.89	[34]
Lead-Zinc-Borate	5.26	4.13	2.48	[26]
Oxy-Fluoro-Borate	1.41	12.11	9.96	[35]
YVO_4	0.812	1.477	1.836	[32]
$GdVO_4$	22.458	4.818	2.182	This work (c-axis)

After obtaining the values of intensity parameter Ω_t, we can calculate the oscillator strength $f_{JJ'}$ between two excited states and the other spectroscopic parameters such as spontaneous radiative transition rate, branching ratio and integrated emission cross section. The main results in the c-axis direction are listed in Table 3.

Table 3. Oscillator strengths, radiative transition rates, branching ratios and integrated emission cross sections between excited states of Ho^{3+} in $Ho^{3+}:GdVO_4$.

Transition	Wavelength/nm	$f^{\mathrm{ed}}_{\mathrm{JJ'}}/10^{-6}$	$f^{\mathrm{md}}_{\mathrm{JJ'}}/10^{-6}$	$A^{\mathrm{ed}}_{\mathrm{JJ'}}/\mathrm{s}^{-1}$	$A^{\mathrm{md}}_{\mathrm{JJ'}}/\mathrm{s}^{-1}$	$\sum A_{\mathrm{JJ'}}$	τ/ms	β	$\sum \mathrm{JJ'}/10^{-18}\mathrm{cm}$
$^5I_7 \rightarrow {}^5I_8$	2047.418	3.126	0.601	193.42	37.17	230.59	4.337	1	3.299
$^5I_6 \rightarrow {}^5I_7$	3005.621	1.829	0.711	52.499	20.425	540.94	1.849	0.13481	2.248
$\rightarrow {}^5I_8$	1195.8	2.580	0	468.01	0			0.86519	2.284
$^5I_5 \rightarrow {}^5I_6$	4046.617	1.45	0.58	22.968	9.187	424.85	2.354	0.07568	1.797
$\rightarrow {}^5I_7$	1674.761	2.431	0	224.75	0			0.52902	2.152
$\rightarrow {}^5I_8$	908.513	0.535	0	167.95	0			0.3953	0.473
$^5I_4 \rightarrow {}^5I_5$	4778.287	1.616	0.381	18.354	4.324	269.51	3.710	0.08415	1.767
$\rightarrow {}^5I_6$	2132.014	1.807	0	103.11	0			0.38258	1.600
$\rightarrow {}^5I_7$	1220.956	0.691	0	120.29	0			0.44634	0.612
$\rightarrow {}^5I_8$	756.087	0.052	0	23.429	0			0.08693	0.046
$^5F_5 \rightarrow {}^5I_6$	1513.661	2.466	0	279.11	0	7500.8	0.133	0.03721	2.183
$\rightarrow {}^5I_7$	989.511	5.779	0	1530.9	0			0.2041	5.116
$\rightarrow {}^5I_8$	660.415	9.534	0	5669.7	0			0.75588	8.440
$^5S_2 \rightarrow {}^5I_4$	2038.819	1.656	0	103.31	0	5992.9	0.167	0.01724	1.466
$\rightarrow {}^5I_5$	1420.253	0.705	0	90.66	0			0.01513	0.624
$\rightarrow {}^5I_6$	1037.495	1.772	0	426.99	0			0.07125	1.569
$\rightarrow {}^5I_7$	761.151	5.097	0	2282	0			0.38078	4.512
$\rightarrow {}^5I_8$	550.237	3.605	0	3088.3	0			0.51533	3.191
$^5F_4 \rightarrow {}^5I_5$	1420.253	2.813	0	361.73	0	12667	0.0789	0.02856	2.490
$\rightarrow {}^5I_6$	1037.495	3.715	0	895.15	0			0.07067	3.289
$\rightarrow {}^5I_7$	761.151	3.145	0	1408.2	0			0.11117	2.784
$\rightarrow {}^5I_8$	550.237	11.538	0	9884.4	0			0.78031	10.214
$^5F_3 \rightarrow {}^5F_5$	2034.629	2.185	0	136.89	0	12042	0.083	0.01137	1.934
$\rightarrow {}^5I_4$	1418.701	2.858	0	368.3	0			0.03058	2.53
$\rightarrow {}^5I_5$	1088.755	3.018	0	660.33	0			0.05483	2.671
$\rightarrow {}^5I_6$	848.752	3.232	0	1163.9	0			0.09665	2.861
$\rightarrow {}^5I_7$	654.365	7.792	0	4719.9	0			0.39194	6.897
$\rightarrow {}^5I_8$	492.174	4.649	0	4977.7	0			0.41335	4.115
$^5F_2 \rightarrow {}^5I_4$	1331.913	3.323	0	485.83	0	8598.7	0.116	0.05650	2.942
$\rightarrow {}^5I_5$	1036.903	3.629	0	875.37	0			0.1018	3.212
$\rightarrow {}^5I_6$	816.86	5.229	0	2032.4	0			0.23636	4.629
$\rightarrow {}^5I_7$	635.243	1.149	0	738.2	0			0.08585	1.017
$\rightarrow {}^5I_8$	481.301	3.922	0	4390.9	0			0.51064	3.471

Table 3 *Continued*

Transition	Wavelength/nm	$f^{ed}_{JJ'}/10^{-6}$	$f^{md}_{JJ'}/10^{-6}$	$A^{ed}_{JJ'}/s^{-1}$	$A^{md}_{JJ'}/s^{-1}$	$\sum A_{JJ'}$	τ/ms	β	$\sum JJ'/10^{-18}$cm
$^3K_8 \rightarrow {}^5I_8$	481.301	2.456	0	2749.5	0	3061.6	0.327	0.89807	2.174
$^5G_6 \rightarrow {}^5F_5$	1570.007	28.247	0	2972.3	0	179990	0.00556	0.01651	25.004
$\rightarrow {}^5I_7$	597.479	16.294	0	11838	0			0.06577	14.423
$\rightarrow {}^5I_8$	459.306	133.33	0	163930	0			0.9108	118.03
$^5F_1 \rightarrow {}^5I_4$	1056.301	4.647	0	1080.2	0	8333.4	0.120	0.12962	4.114
$\rightarrow {}^5I_5$	861.846	8.561	0	2989.5	0			0.35874	7.578
$\rightarrow {}^5I_6$	704.176	5.216	0	2728.1	0			0.32737	4.617
$^5G_5 \rightarrow {}^5F_5$	1220.36	12.807	1.756	2230.5	305.88	68917	0.0145	0.03680	12.892
$\rightarrow {}^5I_6$	663.923	11.251	0	6620.2	0			0.09606	9.960
$\rightarrow {}^5I_7$	538.735	47.077	0	42069	0			0.61042	41.673
$\rightarrow {}^5I_8$	423.783	11.477	0	16575	0			0.24051	10.159
$^5G_4 \rightarrow {}^5F_5$	988.338	3.121	0.012	828.72	3.081	74039	0.0135	0.01124	2.773
$\rightarrow {}^5I_4$	816.193	2.825	0	1099.8	0			0.01485	2.500
$\rightarrow {}^5I_5$	695.024	21.803	0	11708	0			0.15813	19.3
$\rightarrow {}^5I_6$	588.720	62.388	0	46687	0			0.63058	55.226
$\rightarrow {}^5I_7$	488.138	7.317	0	7964.1	0			0.10757	6.477
$\rightarrow {}^5I_8$	391.834	1.452	0	2452.5	0			0.03313	1.285
$^3G_5 \rightarrow {}^5F_3$	1457.004	4.905	0	599.25	0	120100	0.00833	0.00499	4.342
$\rightarrow {}^5F_4$	1129.688	11.605	0	2358.5	0			0.01964	10.272
$\rightarrow {}^5F_5$	835.841	6.885	0.581	2556.1	215.82			0.02308	6.609
$\rightarrow {}^5I_6$	531.011	12.384	0	11391	0			0.09485	10.963
$\rightarrow {}^5I_7$	447.788	72.187	0	93373	0			0.77746	63.9
$\rightarrow {}^5I_8$	365.404	4.219	0	8196.1	0			0.06824	3.735
$^3H_6 \rightarrow {}^5G_5$	2836.718	2.768	0.014	89.206	0.442	63464	0.0158	0.00141	2.462
$\rightarrow {}^5G_6$	1854.875	2.285	3.451	172.26	260.15			0.00681	5.078
$\rightarrow {}^3K_8$	1621.008	6.478	0	639.39	0			0.01008	5.734
$\rightarrow {}^5F_5$	835.841	4.877	0	1810.6	0			0.02853	4.317
$\rightarrow {}^5I_7$	447.788	3.665	0	4740.1	0			0.07469	3.244
$\rightarrow {}^5I_8$	365.404	28.472	0	55308	0			0.87148	25.203

From the results shown in Table 3, we can find that there are many transitions of Ho^{3+} which possess the large oscillator strengths and large radiative transition rates that exceed $500\,s^{-1}$. If a transition has an oscillator strength larger than 10^{-6}, an integrated emission cross section larger than 10^{-18} cm and a relatively large branching ratio together, it may become a channel of the laser radiation.[36] But some of them may become non-radiative transitions because the start level of the transition is very close to the next under level going with multi-phonons relaxation.

From the aspect of branching ratio, except for the ground state $^5I_8$, the metastable levels $^5I_7$ and $^5I_6$ also occupy some proportion as terminal transition state. Some transitions which terminate at these two metastable levels such as $^5G_4 \rightarrow {}^5I_6$ (589 nm), $^5G_4 \rightarrow {}^5I_7$ (488 nm), $^3G_5 \rightarrow {}^5I_7$ (448 nm) and some other transitions from the higher levels can play an important role in the field of up-conversion laser.[37] $^5S_2$ and $^5F_4$ are two important excited states for their intense green luminescence. The large oscillator strength and the integrated emission cross section for the transition of $^5S_2$, $^5F_4 \rightarrow {}^5I_8$ (550 nm), which are more than 10×10^{-6} and 10×10^{-18} cm make this material a candidate of green lasers. In addition, the transition of $^5S_2$, $^5F_4 \rightarrow {}^5I_5$ (1420 nm), could be used for the fibre amplifiers operating in an around 1400 nm band,[38] which deserves to be regarded. Moreover in the red and the blue bands, the transitions $^5F_5 \rightarrow {}^5I_8$ (660 nm) and ($^5F_3$, $^5F_2$, $^3K_8$) $\rightarrow {}^5I_8$ (492 nm, 481 nm) also possess strong abilities to emit, and 2 μm laser sources, which come from the transition $^5I_7 \rightarrow {}^5I_8$ in Ho^{3+} ion doped materials, are potentially useful for a variety of applications. In the $Ho^{3+}:GdVO_4$ crystal, this transition (2047 nm) also has a large enough oscillator strength and a large integrated emission cross section to become the channel of 2 μm laser.

Except for the transitions discussed above, there remain many transitions that have large oscillator strengths and integrated emission cross sections as listed in Table 3. Some of them, starting from metastable levels such as ${}^5F_3 \rightarrow {}^5I_7{}^5I_8$, ${}^5G_5^3G_5 \rightarrow {}^5I_7{}^5I_8$ and ${}^5G_4 \rightarrow {}^5I_6{}^5I_7$, are worth noticing as laser transitions. On the whole, from these analyses, we can say that the $Ho^{3+}:GdVO_4$ crystals have a relatively strong ability to lase.

5. Energy level splitting of Ho^{3+}

The effect of ion central force field and the interaction between spin and orbit of electron make the spectrum items of the rare earth ions in the crystal split into several levels marked by quantum number of total angular momentum (${}^{2s+1}L_J$). In addition, the effect of some other ions that are near to the ion that we discuss makes the levels split into Stark sub-levels further. Because the locations of ions in the crystal field possess symmetry, the Hamiltonian of the ion, which is disturbed by the crystal field, is changeless under the symmetry operation of the location in which we are interested. And the Stark sub-levels, which come from the perturbation of crystal field, have characteristics of the irreducible representation of the point group that the ion possesses. In other words, these Stark levels can be marked by the irreducible representation of that point group, such as ${}^{2s+1}L_{J(\Gamma i)}$, where Γ is the irreducible representation, i is the number from 1 to the number of irreducible representation n.[39]

The Ho^{3+} ions in $Ho^{3+}:GdVO_4$laser crystal replace some of Gd^{3+} ions, and the symmetry of Ho^{3+} belongs to the point group D_{2d}. So we can calculate how many and which irreducible representations constitute the representation of a given level according to the orthogonality theorem equation of group theory and the character tables of symmetric group D_{2d}.[39]

$$\chi^{(j)}(\alpha) = \frac{\sin\left(j+\frac{1}{2}\right)\alpha}{\sin\frac{\alpha}{2}}, \tag{7}$$

where α is the angle of symmetry operations, j is the angular momentum of levels. The result is shown in Fig.4, in which the markers on the left represent levels and on the right refer to the irreducible representations.

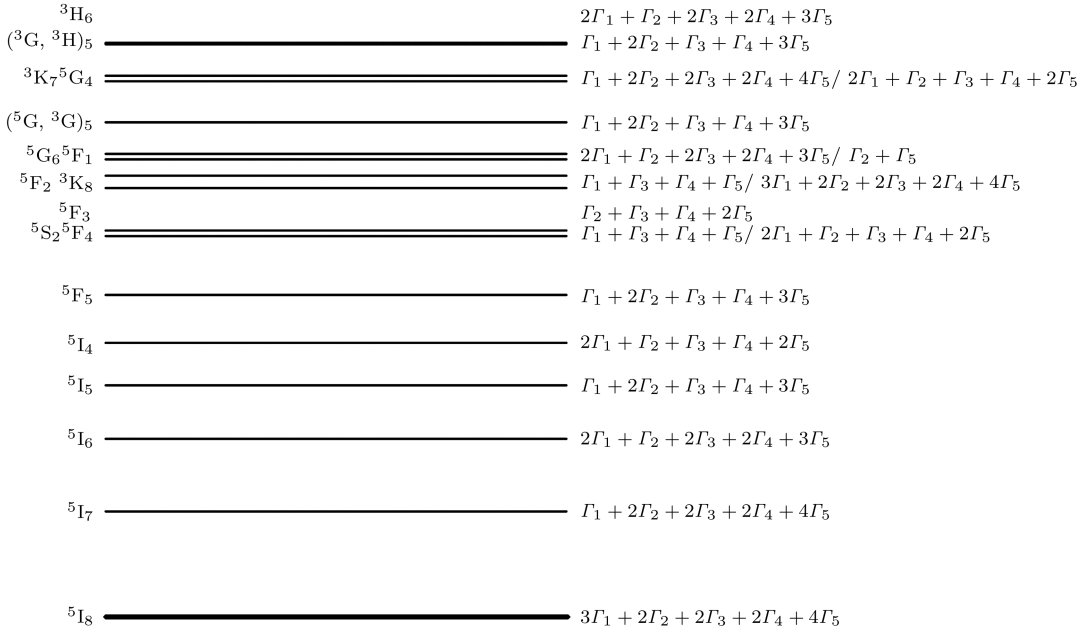


Fig.4. Ho^{3+} energy levels in a Ho^{3+}:$GDVO_4$ crystal.

6. Conclusions

We first measure the absorption spectrum of $Ho^{3+}:GdVO_4$ crystal, and obtain the three intensity parameters of Ho^{3+} ion. And then some optical parameters such as radiative transition rate, branching ratio and integrated emission cross section are calculated. Finally we discuss the splitting of the energy levels of Ho^{3+} in the crystal based on the group theory.

According to the absorption spectrum, we can find that the absorption strengths in the whole range of spectrum are strong, which could result in high pumping efficiency. Especially the absorption intensity of excited state $^5G_6$ is much stronger than that of any other excited state. Meanwhile there are many transitions in the crystal which satisfy the condition of luminescence. For example, $^5F_4{}^5S_2 \rightarrow {}^5I_8$, $^5F_5 \rightarrow {}^5I_8$, $^5I_7 \rightarrow {}^5I_8$, etc are all remarkable and have large oscillator strengths, large integrated emission cross sections and high branching ratios. Moreover $GdVO_4$ crystal has a larger absorption cross section and a larger emission cross-section, and a higher thermal conductivity than YVO_4 crystal and also has many other advantages which are suitable for laser crystal. So as a material of solid state laser in a visible light range at a wavelength of 2 μm, the Ho^{3+}:$GdVO_4$ crystal has a good prospect.

Acknowledgment

Authors would like to thank Professor Aihua Gao (Institute of Physics, Chinese Academy of Sciences) for his cooperation and also Physcience Optoelectronics Co. Ltd Beijing for the support.

References

[1] Chen X B, Zhang G Y, Wang H, Liu Y B, Chen J K, Shang M R and Li J W 1993 *Acta Phys. Sin.* (Overseas Edition) **2** 771
[2] Chen X B, Zheng J and Song Z F 2001 *Chin. Phys.* **10** 1163
[3] Wang J G, Zhang Z G, Xu J Z, Xu J R, Fu P M and Chen X B 2000 *Chin. Phys.* **9** 210
[4] Xiao S G, Yang X L and Liu Z W 2002 *Chin. Phys.* **11** 188
[5] Huang L L, Fu Y B and Wu L N 2003 *Chin. Phys.* **12** 1417
[6] Yang D L, Hou Y Y, Zhao X, Liu G S, Lin H, Liu K and Pun E Y B 2006 *Acta Phys. Sin.* **55** 4304 (in Chinese)
[7] Hao Z, Chen X B, Hou Y B, Song F, Wang H and Zhang G Y 1997 *Acta Phys. Sin.* **46** 1206 (in Chinese)
[8] Chen X B, Song Z F and Nie Y X 1999 *Acta Phys. Sin.* (Overseas Edition) **8** 216
[9] Zhou B K, Gao Y Z and Chen Z R 2004 *Laser Principle* (Beijing: National Defence Industry Press)
[10] Storm M E 1991 *Laser Focus World* **27** 117
[11] Wen L, Zhang L Y, Yang J H, Wang G N, Chen W and Hu L L 2006 *Acta Phys. Sin.* **55** 1486 (in Chinese)
[12] Yang J H, Ma S C and Xu Y 2008 *Chin. Phys.* B **17** 710
[13] Wang Y S, Zhang X Q, Zhang G Y, Liu J, Li Z F, Li J, Xiong G N, Xu Z, Xu X R and Wang J Y 1996 *Acta Phys. Sin.* **45** 635 (in Chinese)
[14] Song F, Su J, Tan H, Shang M R, Wu Z H, Tian J G, Zhang G Y, Cheng Z X and Chen H C 2004 *Acta Phys. Sin.* **53** 3591 (in Chinese)
[15] Sun Y X, Gong Q H and Zhou X H 1995 *Acta Phys. Sin.* **44** 872 (in Chinese)
[16] Yang P, Li S F, Zhang Q Y, Li Y G and Lei X 2007 *Acta Phys. Sin.* **56** 7286 (in Chinese)
[17] Yuan F C, Ran G Z, Chen Y, Zhang B R, Qiao Y P, Fu J S, Qin G G, Ma Z C and Zong W H 2001 *Acta Phys. Sin.* **50** 2487 (in Chinese)
[18] Zaguniennyi A I, Ostoumov V G, Shcherbakov I A, Jensen T, Meyn J P and Huber G 1992 *Sov. J. Quant. Electron.* **22** 1071
[19] Zhang C, Wei Z Y, Zhang L, Zhang C Y and Zhang Z G 2006 *Chin. Phys.* **15** 2606
[20] Judd B R 1962 *Phys. Rev.* **127** 750
[21] Ofelt G S 1962 *J. Chem. Phys.* **37** 511
[22] Kaminskii A A 1981 *Laser Crystals* (New York: Springer-Verlag)
[23] Carnall W T, Fields P R and Wybourne B G 1965 *J. Chem.Phys.* **42** 3797
[24] Zhang S Y and Bi X Z 1991 *Spectroscopy Theory of Rare Earth* (Changchun: Jilin Science and Technology Press) (in Chinese)
[25] Rajnak K and Krupke W F 1967 *J. Chem.Phys.* **46** 3532
[26] Hussain N S, Ali N, Dias A G, Lopes M A, Santos J D and Buddhudu S 2006 *Thin Solid Films.* **515** 318
[27] Jørgensen C K and Reisfeld R 1983 *J. Less-Common Met.* **93** 107
[28] Yang W Q, Wu M Q, Chen J K and Zhuang J 2001 *Spectrosc. Spect. Anal.* **21** 28
[29] Yang Y M, Yao B Q, Chen B J, Wang C, Ren G Z and Wang X J 2007 *Opt. Mater.* **29** 1159
[30] Xu W W, Xu X D, Wang J Y, Wu F, Su L B, Zhao G J, Zhao Z W, Zhou G Q and Xu J 2008 *J. Alloys.Compd.* (in press)
[31] Lomheim T S and Deshazer L G 1978 *J. Appl. Phys.* **49** 5517
[32] Wang H Y, Li J F, Jia G H, You Z Y, Yang F G, Wei Y P, Wang Y, Zhu Z J, Liu X A and Tu C Y 2007 *J. Alloys. Compd.* **431** 277
[33] Lorenzo A, Baussa L E, SanzGarcia J A and GarciaSole J 1996 *J. Phys. Condens. Mater.* **8** 5781
[34] Malinowski M, Frukacz Z, Szuflinska M, Wnuk A and Kaczkan M 2001 *J. Alloys. Compd.* **300** 389
[35] Rai S B 2002 *Spectrochimica. Acta A.* **58** 1559
[36] Caird J, DeShazer L and Nella J 1975 *IEEE J. Quant. Electro.* **QE-11** 874
[37] Deren P, Goldner P and Guillot-Noel O 2006 *J. Lumin.* **119** 38
[38] Choi Y G, Park B J and Kim K H 2002 *Chem. Phys. Lett.* **354** 69
[39] Song Z F 1987 *The Theory and Application of Atom Spectroscopy and Crystal Spectroscopy* (Beijing: Science Press) (in Chinese)